Hole-to-surface resistivity measurements

at Gibson Dome (drill hole GD-1),

Paradox Basin, Utah

by

Jeffrey J. Daniels

Abstract

Field measurements over the sand, shale, evaporite sequence at Gibson Dome illustrate procedures for gathering, reducing, and qualitatively interpreting hole-to-surface resistivity data. The magnitude and direction of the total electric field resulting from a current source placed in a drill hole is calculated from ~~outlog and~~ potential difference measurements for a grid of closely-spaced stations. A contour map of these data provides a detailed map of the distribution of the electric field away from the drill hole. Computation of the apparent resistivity from the total electric field helps to interpret the data with respect to the ideal situation of a layered earth. Repeating the surface measurements for different source depths gives an indication of variations in the geoelectric section with depth.

The presence of a conductive borehole fluid hinders the quantitative interpretation of the field data. However, a qualitative interpretation of the field data indicates the geoelectric section around drill hole GD-1 is not perfectly layered. The geoelectric section appears to dip to the northwest, and contains anomalies in the resistivity distribution that may be representative of localized thickening or folding of the salt layers.

Introduction

The geology in the vicinity of nuclear waste repositories must be evaluated without extensive drilling that might destroy the structural integrity of the rocks near the mined area. Hole-to-surface and hole-to-hole geophysical measurements can be useful techniques for determining the presence of geologic inhomogeneities away from a drill hole.

Hole-to-surface direct current resistivity measurements are made by placing a pole or bipole source down a borehole and measuring the resulting distribution of the electric potential on the surface. Theoretical studies of surface potentials due to in-hole current sources have been described by Alfano (1962), Merkel (1971), Merkel and Alexander (1971), Snyder and Merkel (1973), and Daniels (1977, 1978).

Field studies conducted previously at Salt Valley (Daniels, and Scott 1980) indicated the feasibility of making hole-to-surface resistivity measurements over an evaporite sequence. However, the Salt Valley study was conducted using single component electric field measurements, which were shown in a subsequent study (Daniels, 1981) to be less diagnostic of local geologic inhomogeneities than total electric field measurements.

The source-receiver configuration used in this study is shown in figure 1. The current source consisted of a current "sink" at the casing collar, and a current "source" at depth. Ideally, the current "sink" should be placed a large distance from the source hole. However, due to the depth of drill hole GD-1 it was impractical to place the current "sink" away from the drill hole.

A dipole potential receiver, consisting of closely spaced poles, enables the interpreter to calculate the approximate total electric fields. The non-
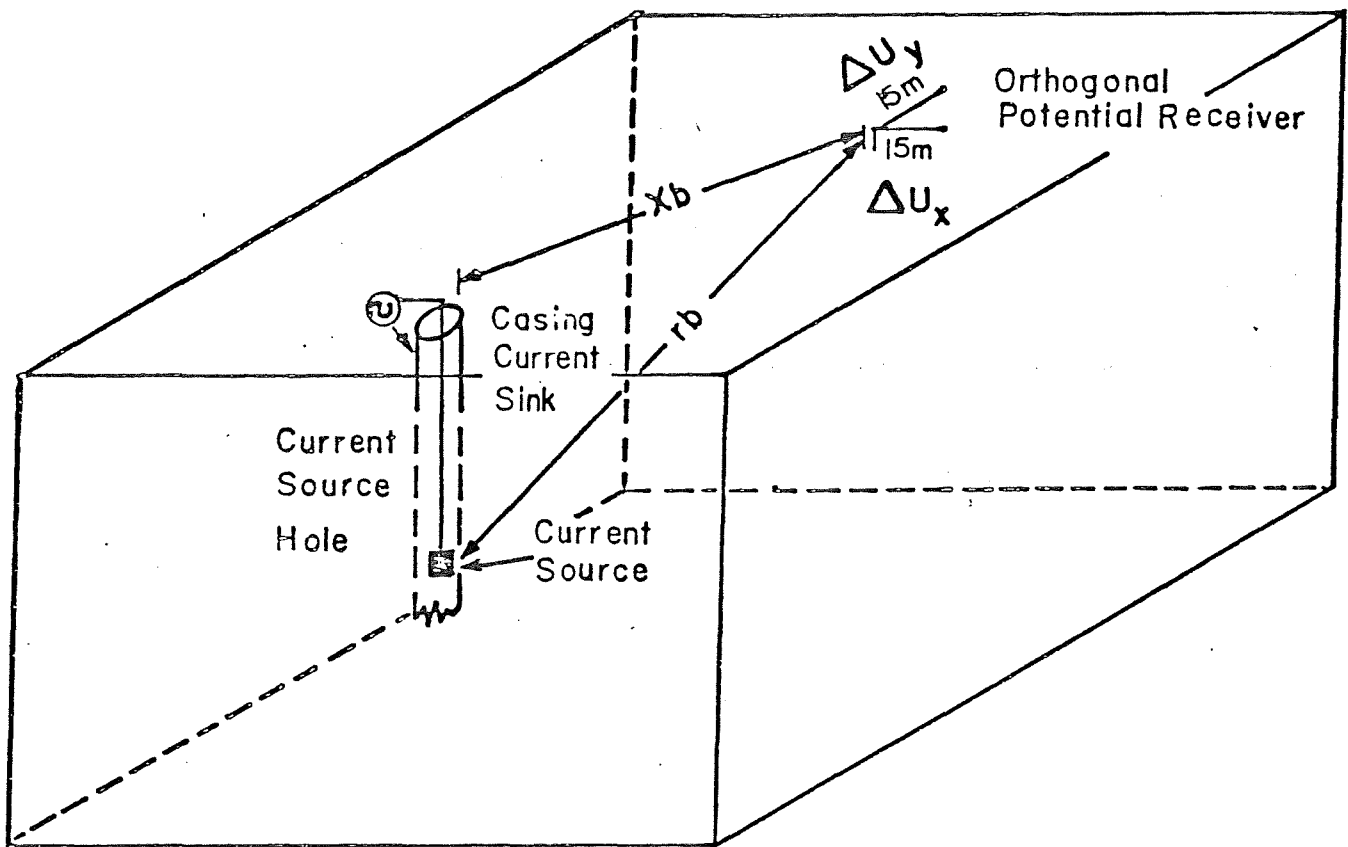
Figure 1.--Field measurement configuration. The total electric field is calculated from the orthogonal dipole potential measurements. (E_t = $((\Delta U_x/15)^2 + (\Delta U_y/15)^2)^{1/2}$). The distances X_b, r_b, and X_a (r_a = X_a) are used in the apparent resistivity calculation.

radial components of the electric field are zero in a homogeneous or a later-
ally isotropic earth. However, when lateral inhomogeneities are present in
the geoelectric section, the direction of the electric current emanating from
a buried current source is not radial, and it is necessary to measure two or-
thogonal components of the potential in order to measure the total electric
field. The direction of the total electric field can be computed from orthog-
onal potential dipole measurements by maintaining a consistent orientation and
polarity of the receiver.

Total electric field surface measurements were made using three different
source depths (518 m, 762 m, and 1524 m) in drill hole GD-1 at Gibson Dome.
These measurements were made along lines radial to the source hole at 20°
intervals. The location of drill hole GD-1 and the measurement lines are
shown in figure 2.

Reduction and analysis of field data

Contour maps of the magnitude and direction lines of the total electric
field are shown in figures 3, 4, and 5 for current sources at depths of 518 m,
762 m, and 1524 m, respectively. The magnitude of the total electric field
was calculated using the equation $E_t = (E_x^2 + E_y^2)^{1/2}$, where E_x and E_y are the
orthogonal electric field components calculated by dividing the measured
dipole potential by the receiver dipole length (15 m). The direction of the
total electric field vector was calculated by computing the inverse tangent of
the orthogonal electric field components.

Electric field measurements for each of the source depths show a general-
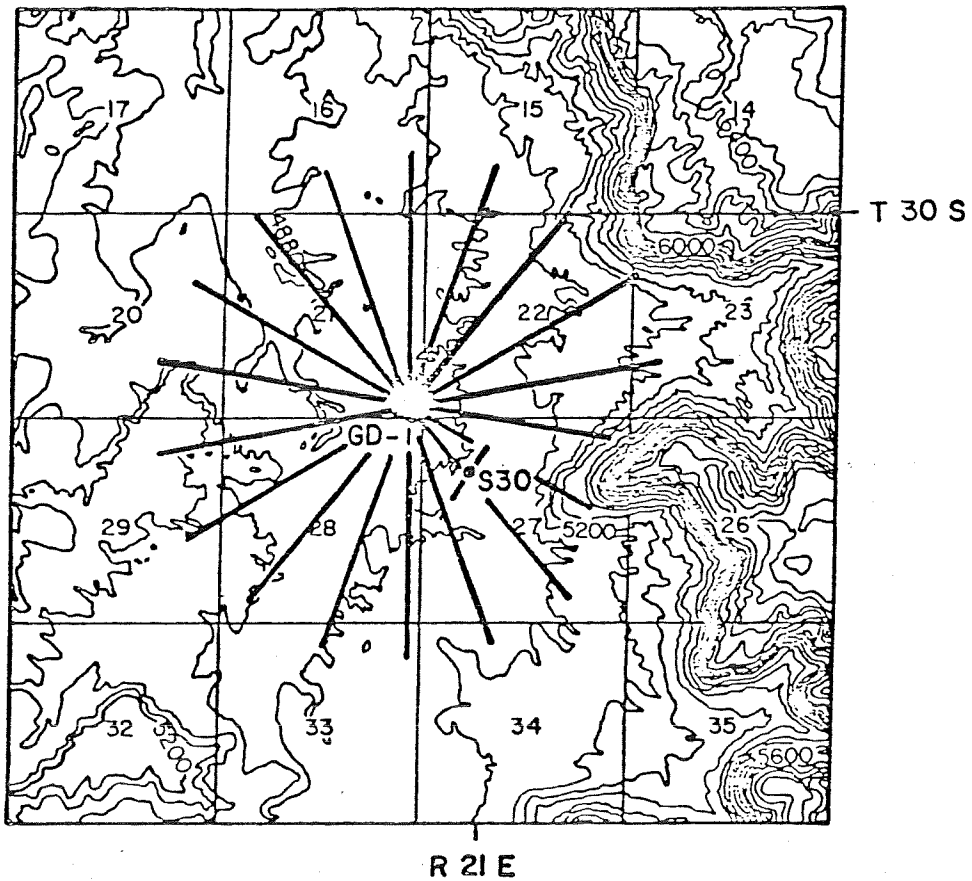ly radial distribution of the direction of the electric field array from the

Figure 2.--Location map for drill hole GD-1, with topographic contours. Measurement lines for data in this study are shown radiating from drill hole GD-1. Topographic contours are in feet (1 ft. = 0.3048 m).
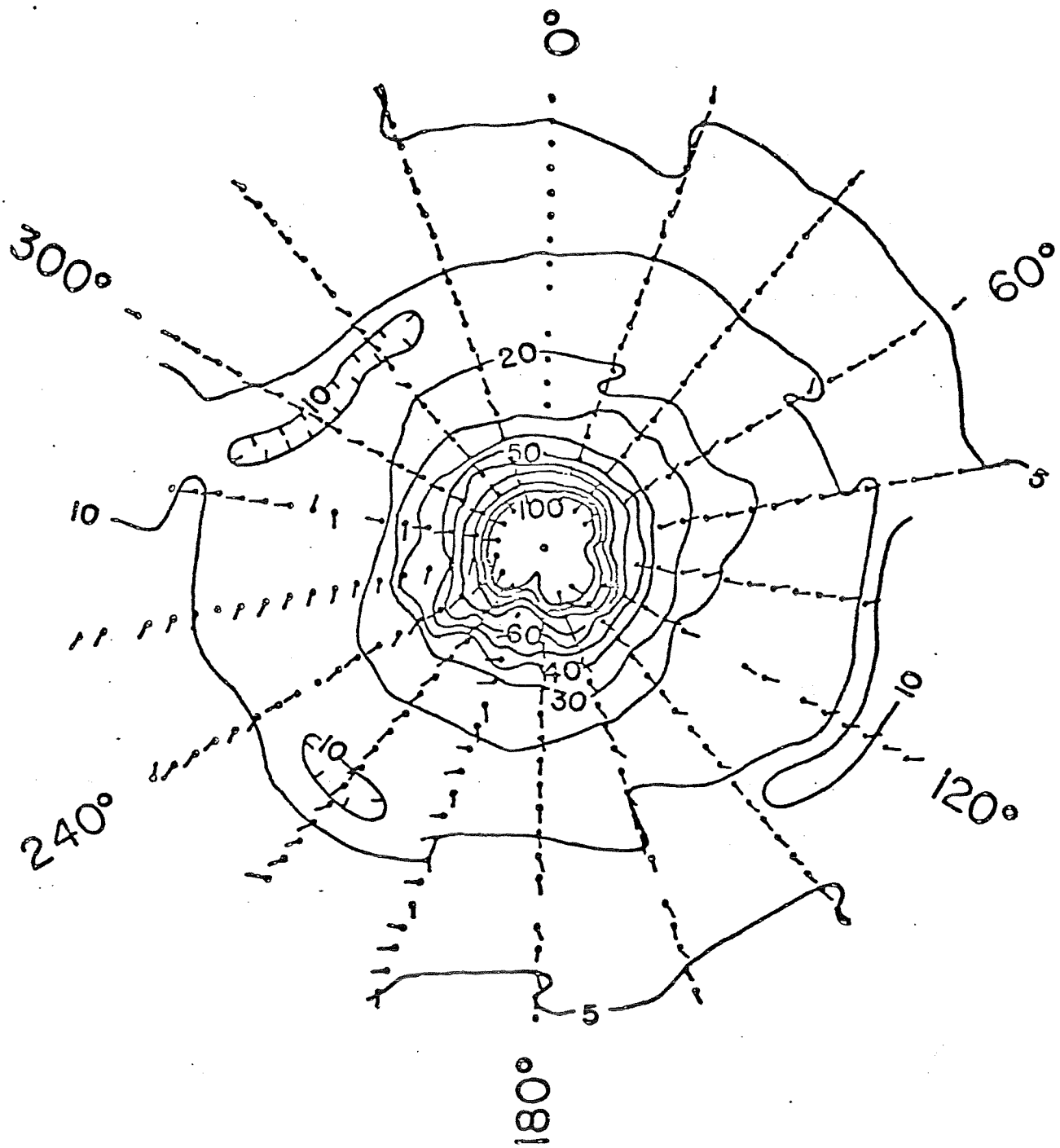
Figure 3.—Contour map of the magnitude of the total electric field divided by
the source current for the current source at a depth of 518 m. The
direction of the total electric field is shown by lines originating
at the measurement station location (indicated by "."). Units for
the plotted values are $V \cdot 10^6 / (A \cdot m)$.

drill hole containing the current source, and a nearly circumferential contour
pattern of the magnitude near the source holes. Deviations from the fields
expected for a laterally isotropic earth include low electric field anomalies
at a distance of 500-to-600 m from the source along the 300° line for source
depths of 518 m and 762 m (figures 3 and 4, respectively). A high electric
field anomaly dominates the response along the 20° line for a source depth of
1524 m (figure 5). The interpretation of these anomalies will be discussed
later in this report.

The apparent resistivity is calculated from the total electric field
using the formula:

$$\rho_a = E_t \left(\frac{2\Pi}{I} \right) \left\{ \frac{1}{X_b^4} + \frac{X_b^2}{r_b^6} + \frac{2}{X_b r_b^3} \right\}^{-1/2}$$

where I is the input current, r_b is the total distance between the "B" current
source and the receiver, and X_b is the surface projection of r_b. The geomet-
ric correction for the apparent resistivity calculation is a radially symmet-
ric factor that can enhance electric field contour patterns tha trend circum-
ferential to the source hole, and diminish patterns that trend radially to the
source hole. Calculating the apparent resistivity from the total electric
field can aid qualitative interpretation when the primary geoelectric section
consists primarily of a laterally isotropic media.

Apparent resistivity contour maps for each of the three source depths are
shown in figures 6, 7, and 8 for source depths of 518 m, 762 m, and 1524 m,
respectively. These resistivity contour maps show a less circumferentially
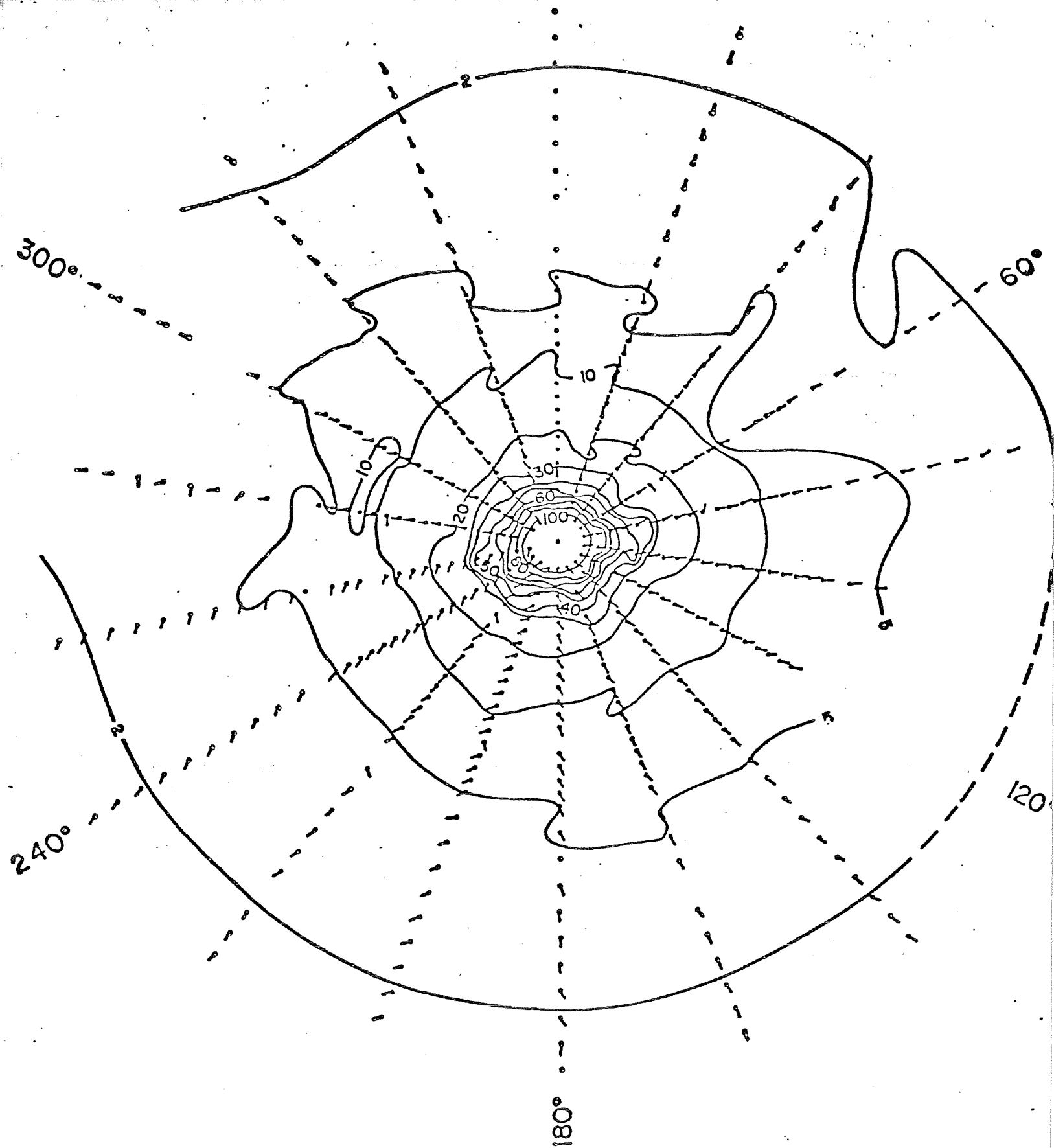symmetric pattern than the corresponding electric field contour maps (figures

Figure 4.—Contour map of the magnitude of the total electric field divided by

the source current for the current source at a depth of 762 m. The

direction of the total electric field is shown by lines originating

at the measurement station location (indicated by dot ".")。 Units
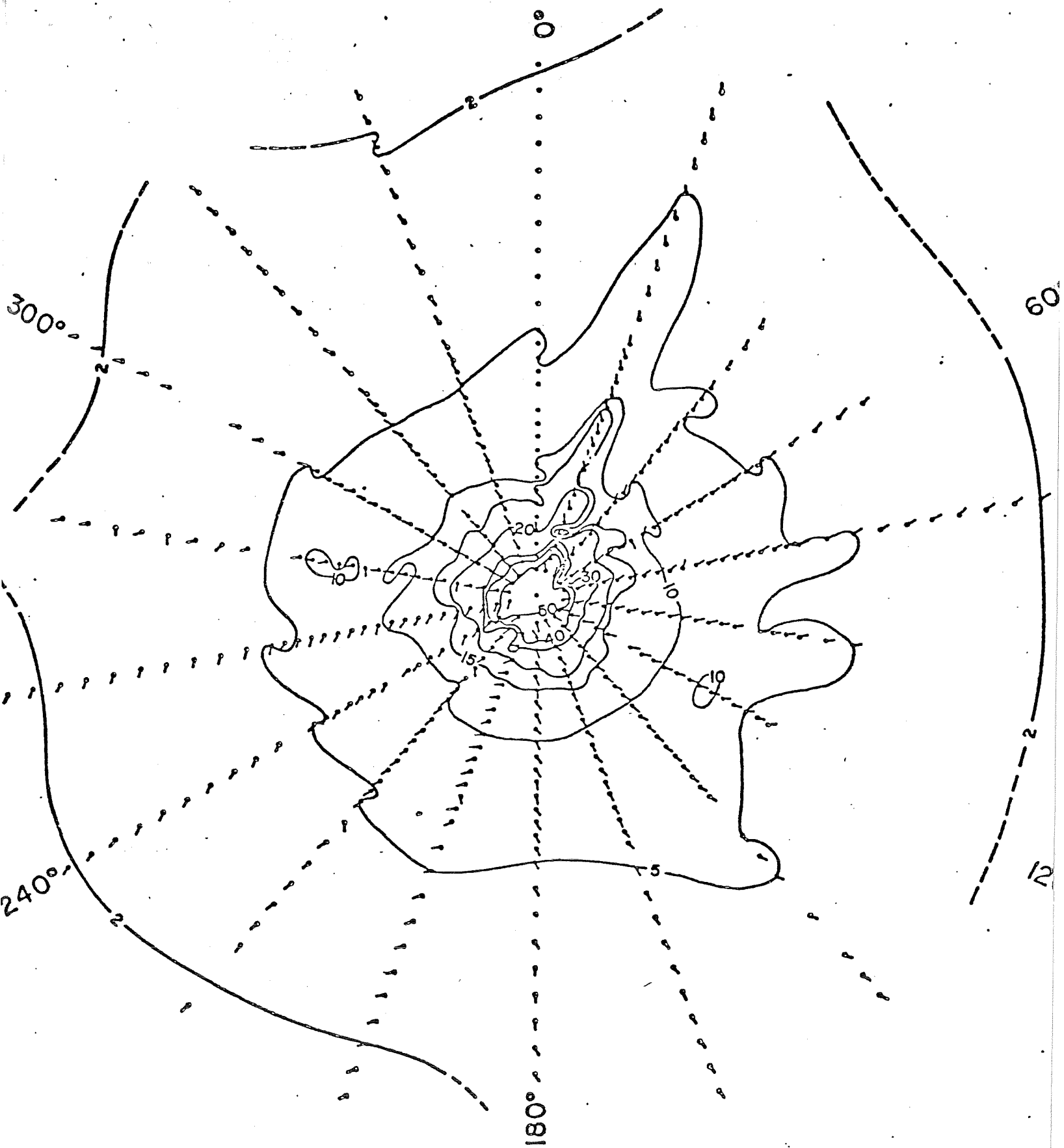
for the plotted values are

Figure 5.—Contour map of the magnitude of the total electric field divided by

the source current for the current source at a depth of 1524 m.

The direction of the total electric field is shown by lines origi-

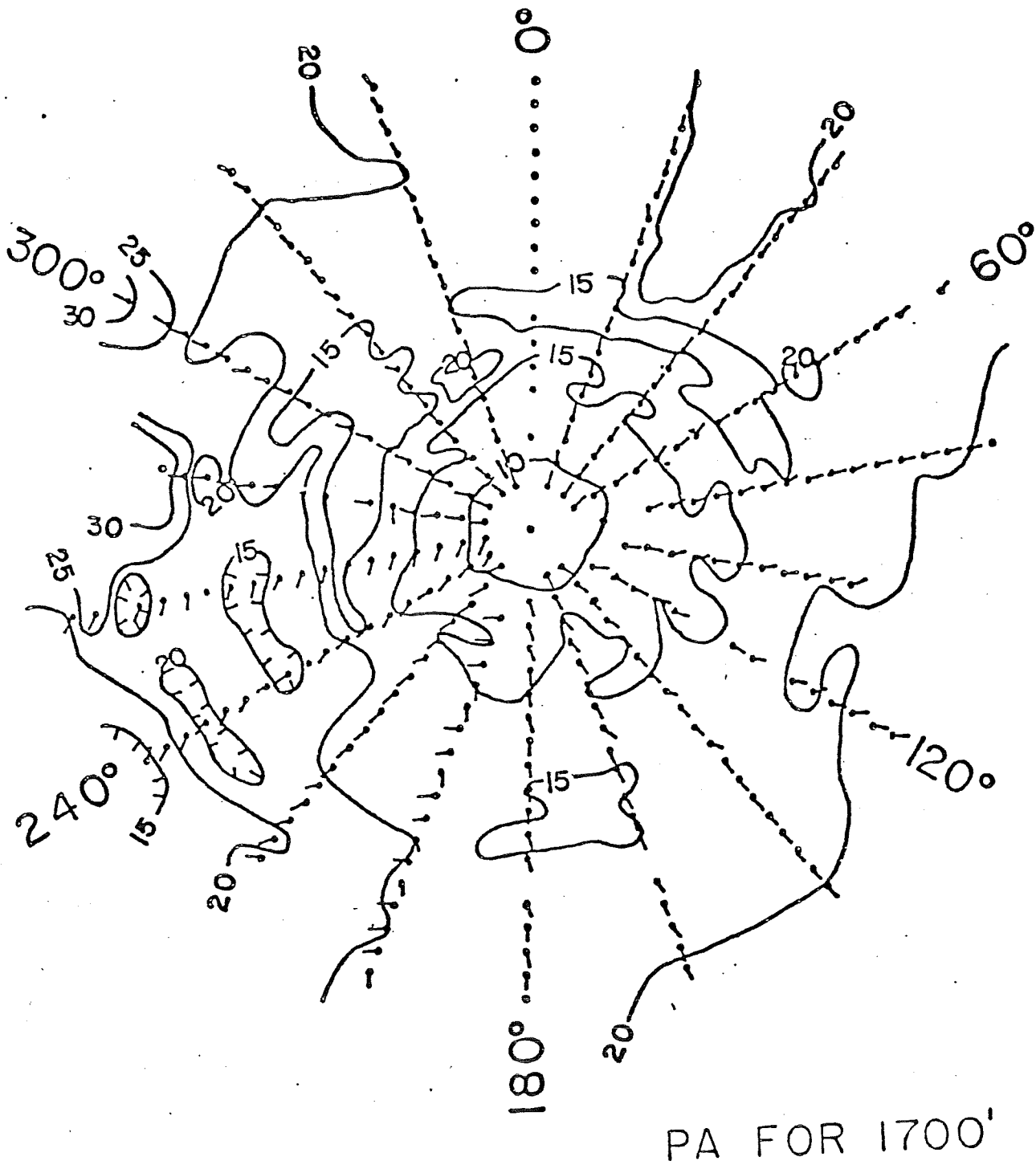nating at the measurement station location (indicated by dots

Figure 6.--Contour map of apparent resistivity (in ohm-m) for the current
source depth of 518 m. Drill hole location is indicated by an "X".
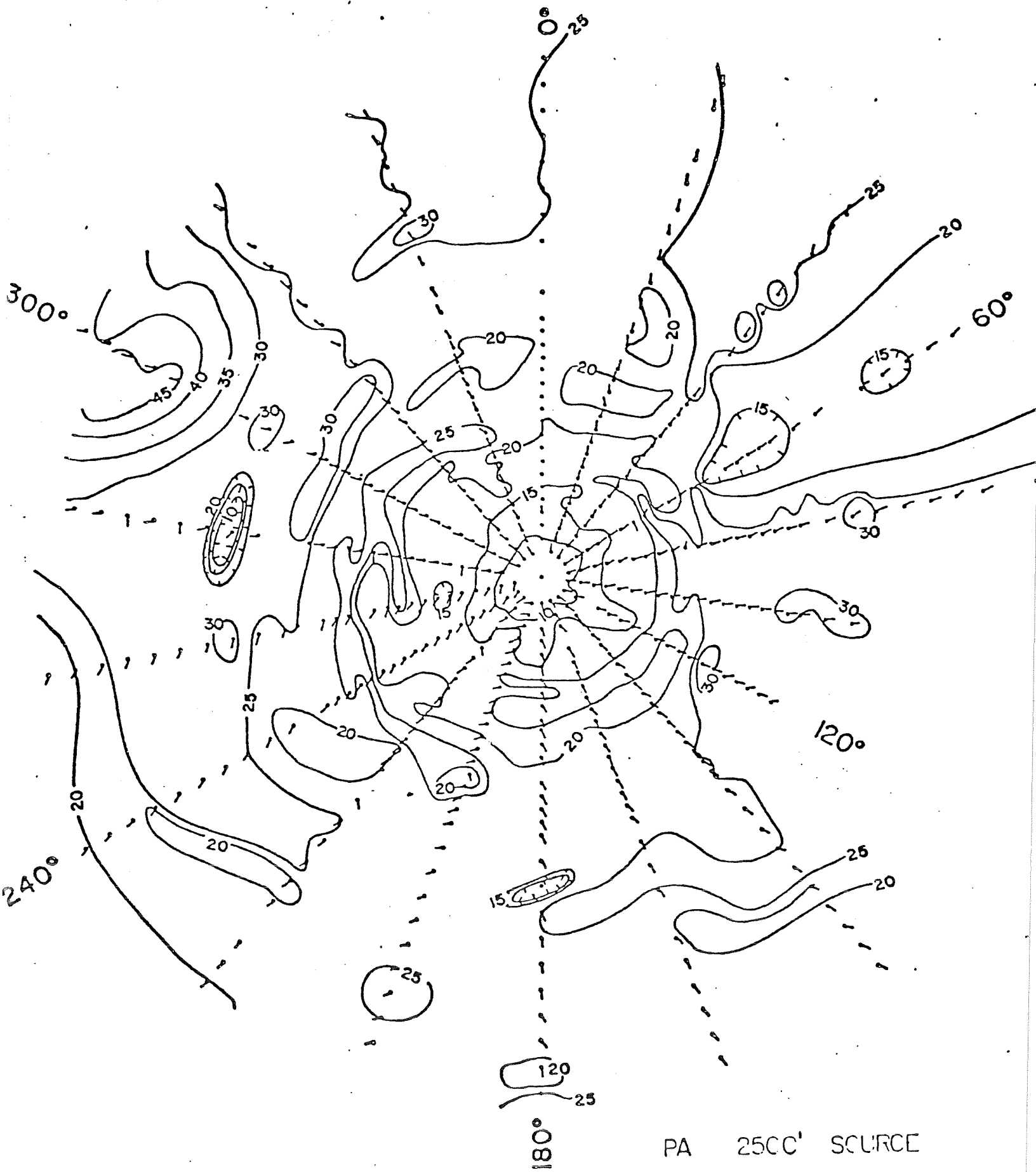
Figure 7.—Contour map of apparent resistivity (in ohm-m) for the current source depth of 762 m. The location of drill hole GD-1 is indicat-
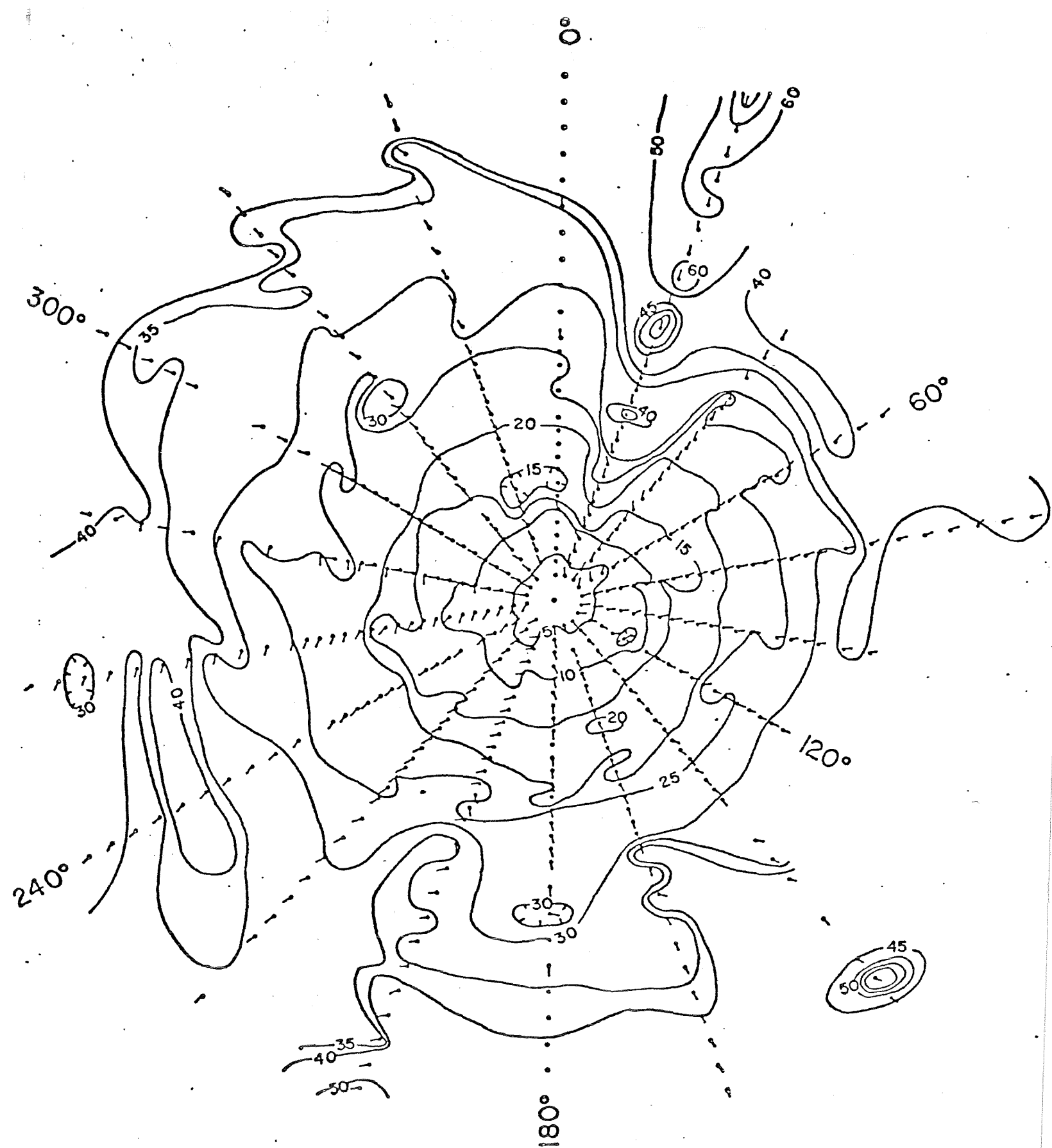
Figure 8.—Contour map of apparent resistivity (in ohm-m) for the current
source depth of 1524 m. The location of drill hole GD-1 is indi-
cated by an "X".

3, 4, and 5). However, the basic contour pattern is approximately that of a laterally isotropic medium. An anomalous region, containing both resistivity highs and lows is present in the vicinity of the 220°-to-300° lines for distances greater than 1000 m for source depths of 518 m and 762 m (figures 6 and 7, respectively). Anomalies in this region are nearly absent for a source depth of 1524 m (figure 8). An interruption in the contour pattern also is present in the vicinity of 160°-to-200° for source depths of 518 m (figure 6) and 762 m (figure 7), indicating the possible presence of a shallow conductive zone. The lines from approximately 0°-to-80° contain zones of anomalously high resistivity values for each of three source depths. The possible geologic cause of these anomalies will be discussed later in this paper.

Layered interpretation of field data

Geophysical well logs and core analysis (Bob Hite, personal communication, May, 1981) from each of the source depths in the study indicates the presence of a layered stratigraphic and geoelectric section. Profiles from the resistivity contour maps in figures 6, 7, and 8 are shown in figure 9 along with a layered earth model and the corresponding model response for source depths of 518 m, 762 m, and 1524 m. The depth of the interface between layers 4 and 5 is approximately equal to the depth of the first salt in drill hole GD-1. The layered sequence chosen for the hole-to-surface model is approximately the same as the Schlumberger resistivity sounding curve for this area, which is shown in figure 10.

A residual apparent resistivity map is obtained by subtracting the layered earth model response from the field data. Residual maps for the three
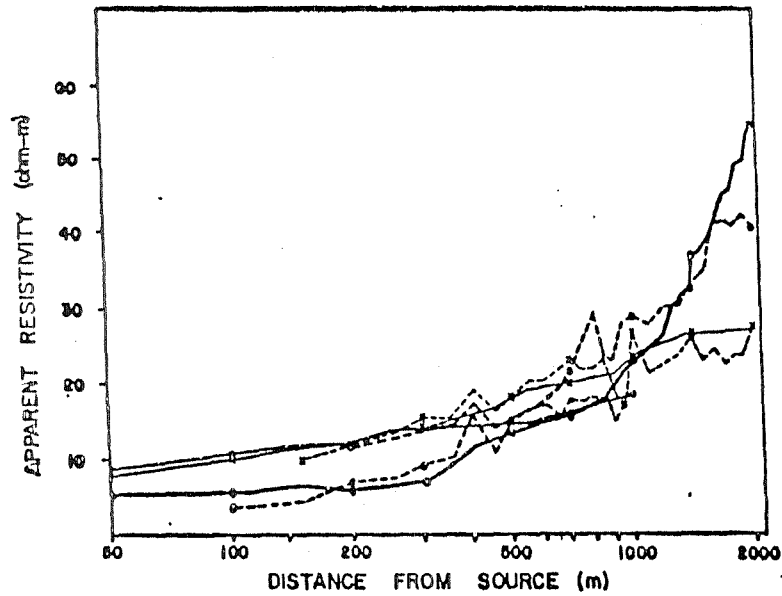
SOURCE DEPTH | LINE | SYMBOL
518 m | 0 | o
762 m | 0 | x
1524 m | 0 | •

(a) Field data and model response for line 0°.
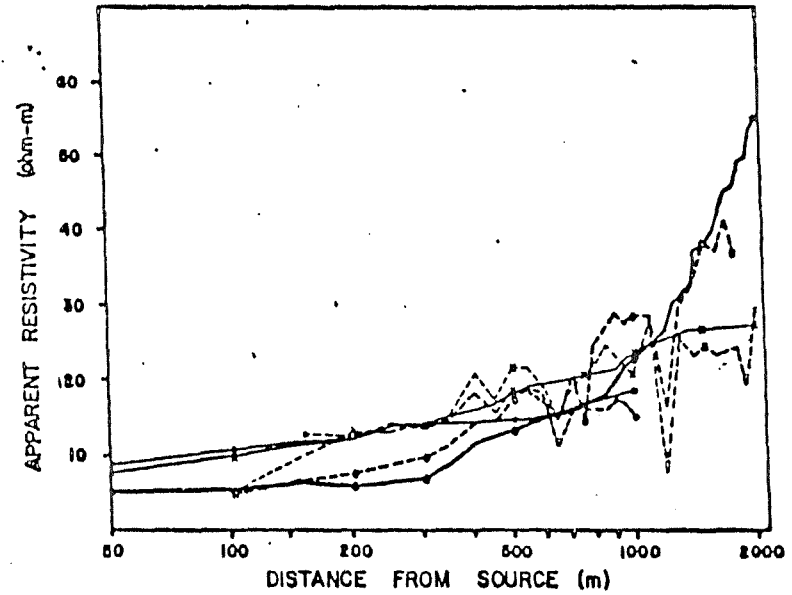
SOURCE DEPTH | LINE | SYMBOL
518 m | 180 | o
762 m | 180 | x
1524 m | 180 | •

(b) Field data and model response for line 180°

Model (518m)

Layer	Resistivity (ohm-m)	Thickness (m)
1	10	20
2	13	180
3	33	200
4	106	500
5	355	800
6	15	∞

Model (762m)

Layer	Resistivity ohm-m	Thickness
1	9	20
2	12	180
3	52	200
4	52	500
5	370	800
6	19	∞

Layer	Resistivity Ohm-m	Thickness
1	8	20
2	5	180
3	65	200
4	120	500
5	191	800
6	18	∞

Figure 9.—Apparent resistivity profiles, layered earth model, and model responses. Field data profiles are from lines 0° (a) and 180° (b).
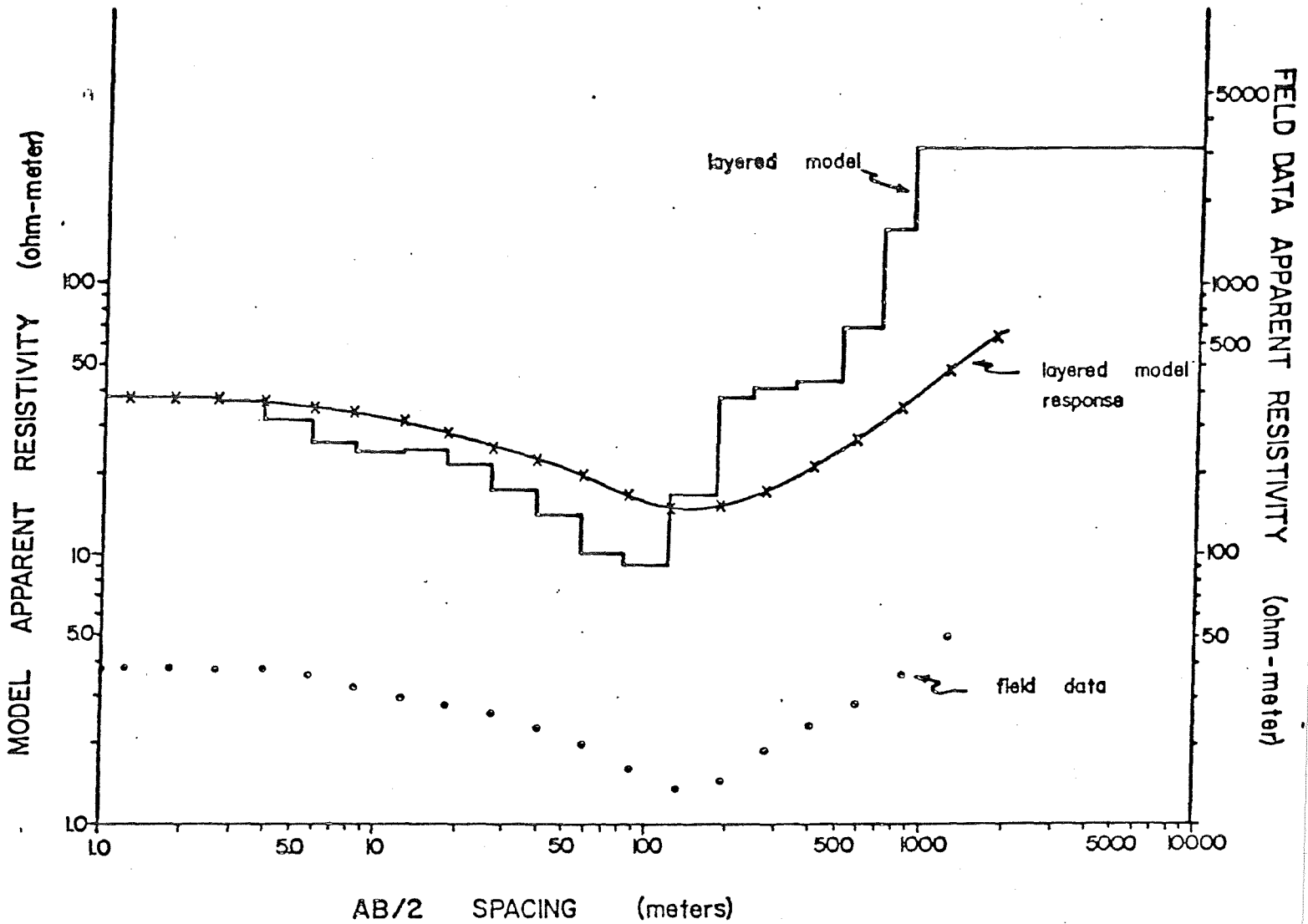
Figure 10.--Schlumberger sounding field data (indicated as "."), interpreted
layered earth model (heavy line) and layered earth model response
for sounding near drill hole GD-1 (Ray Watts and Bob Bisdorf,
personal communication, May, 1981).

source depths discussed in this paper are shown in figures 11, 12, and 13. Regions on the residual maps that have values near-zero are zones where the layered earth model fits the field data.

Subtraction reduction of resistivity data

Different source depths should yield apparent resistivity values that are indicative of the geoelectric section at different depths. Given a measurement from a shallow source and a deep source, the response from the deeper source will reflect the geoelectric section above the shallower source in addition to the geoelectric section between the shallower source and the deeper source. Subtracting the response values for the deep source from the values for the shallow source should enhance the deeper anomalies. Since the response from different source depths are not simple additive functions, this calculation will only give an approximate, and qualitative, estimate of the geoelectric section between the two source depths.

Subtraction-reduction contour maps for source depths of 518 m-to-762 m, and 762 m-to-1524 m are shown in figures 14 and 15, respectively. The resistivity subtraction-reduction in figure 14 illustrates that there is very little difference between the resistivity responses for the two shallow sources. Both of these sources are above the first major high resistivity salt, and the resulting surface measurements are primarily influenced by the same shallow sedimentary geoelectric section. In contrast, the geoelectric section between the 762 m and 1524 m source depths includes several high resistivity salt layers and low resistivity interbed zones. The subtraction-reduction for the 762 m and 1524 m source depths (figure 15) shows a variety
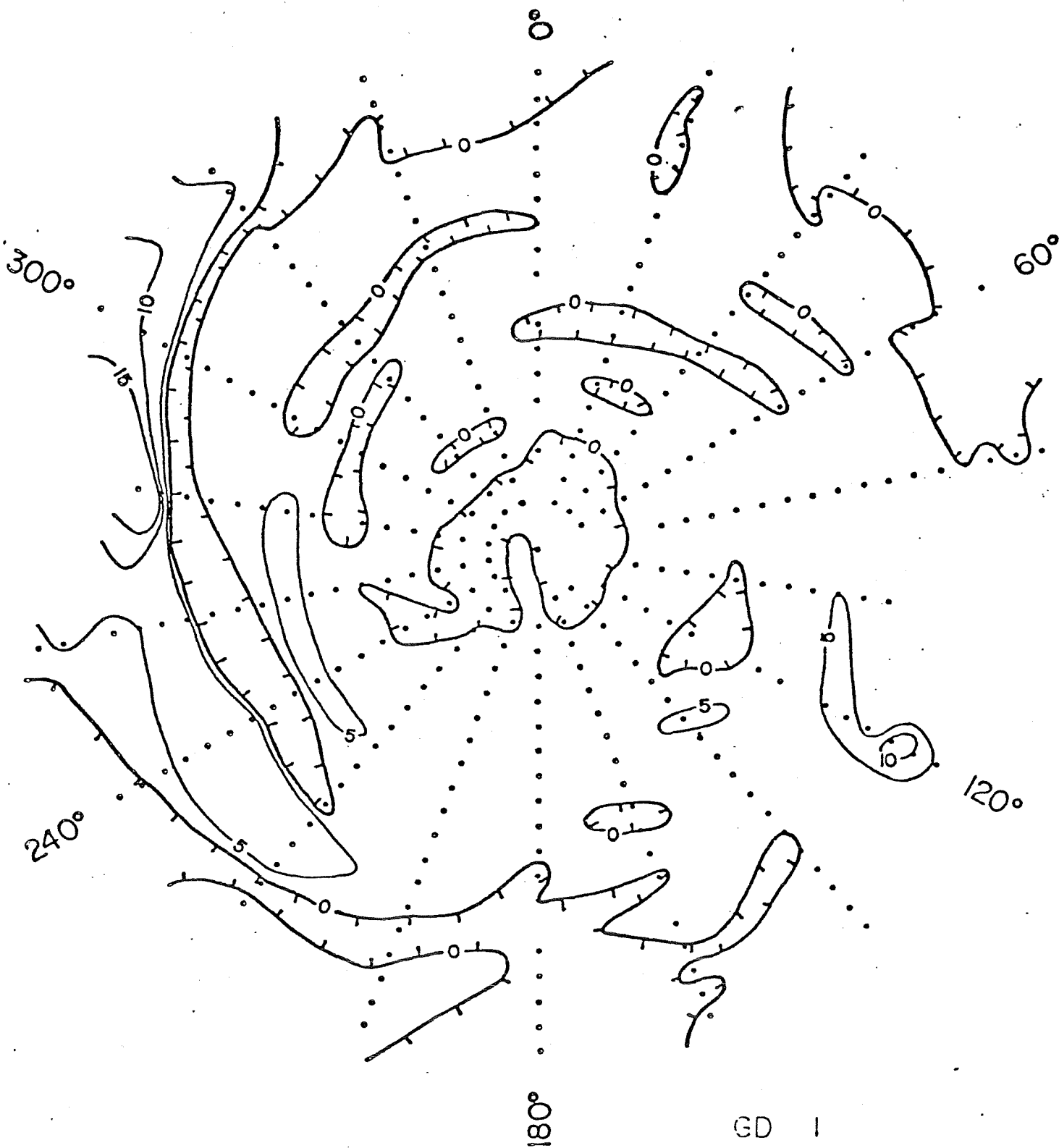
Figure 11.--Residual apparent resistivity contour map (field data-model response, in ohm-m) for source hole GD-1 with the current source at a depth of 518 m.
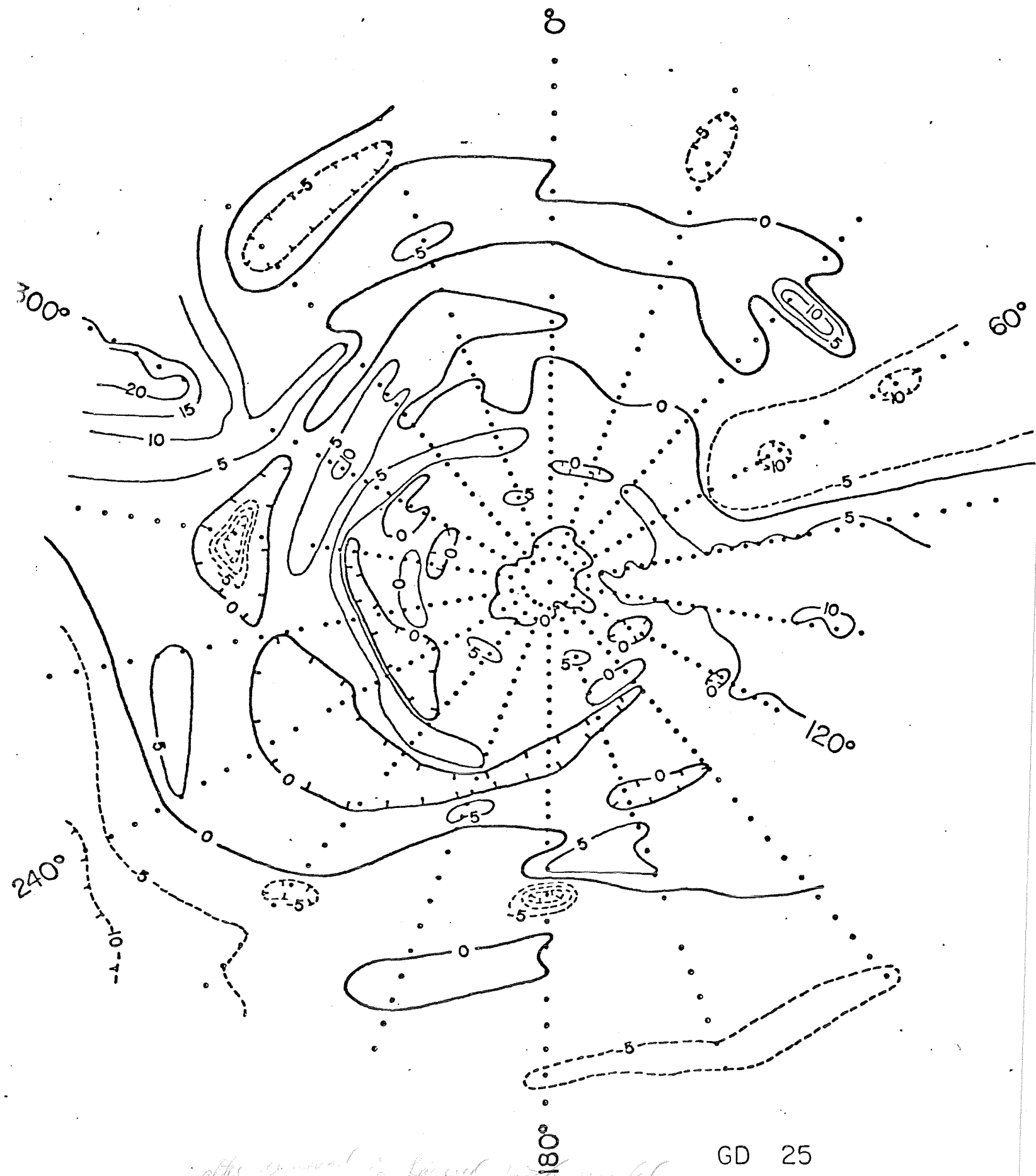
GD 25

Figure 12.—Residual apparent resistivity contour map (field data-model re-
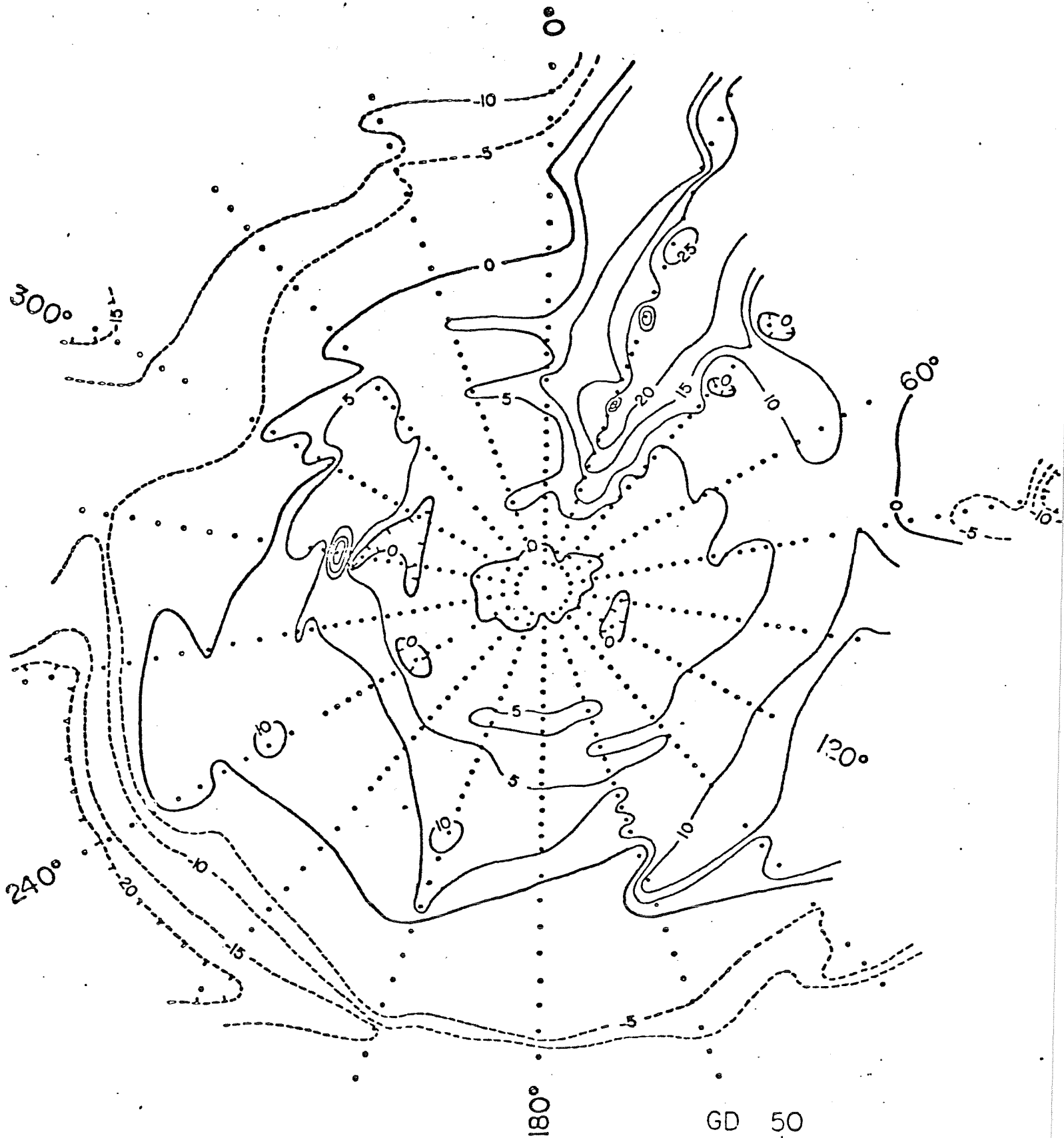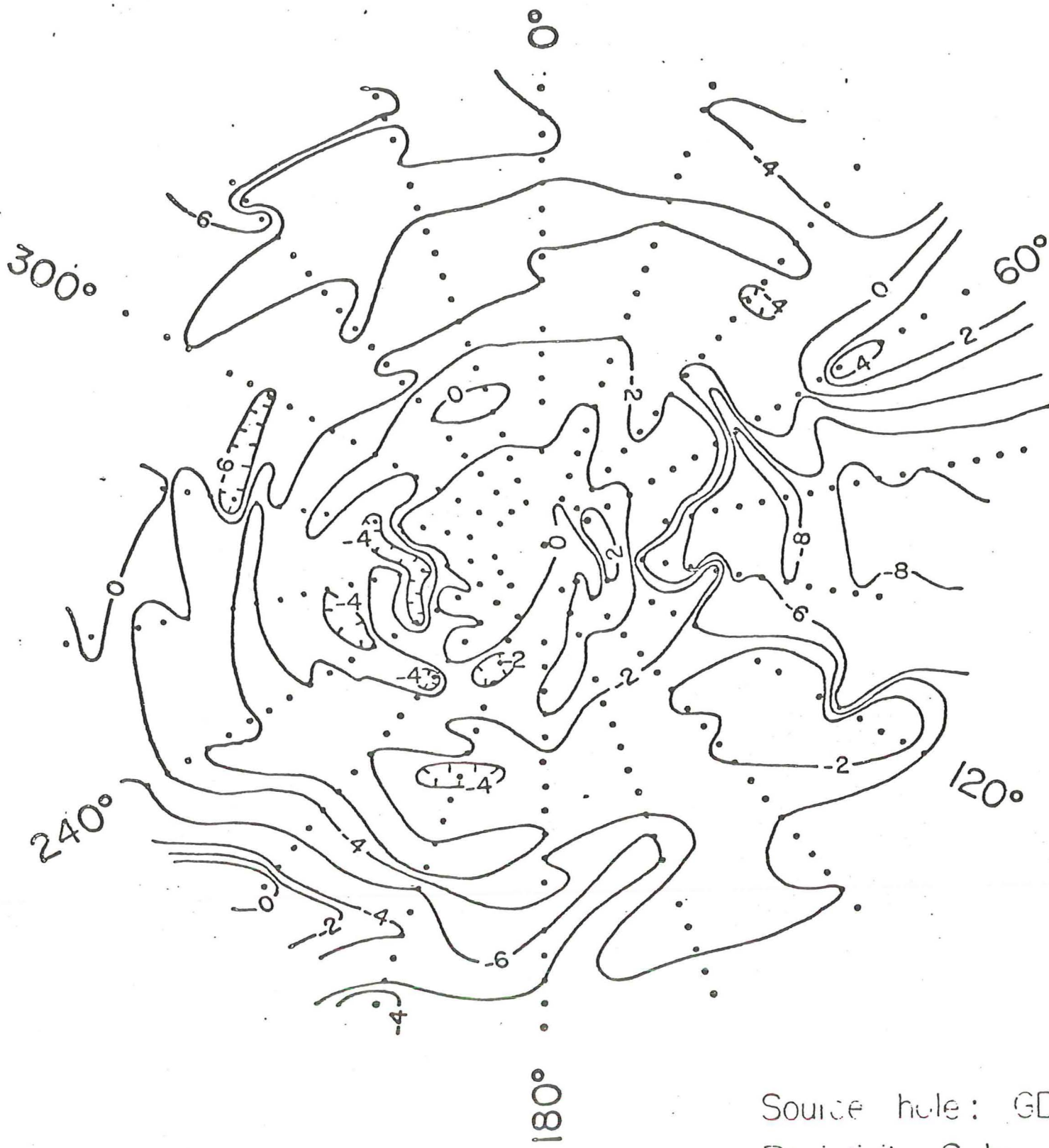sponse, in ohm-m) for source hole GD-1 with the current source at

Figure 13.—Residual apparent resistivity contour map (field data-model response, in ohm-m) for source hole GD-1 with the current source at a depth of 1524 m.

Figure 14.—Resistivity subtraction—reduction contour map for source depths of
518 m and 762 m. Contour values are computed by subtracting the
apparent resistivity values for the 762 m source depth from the
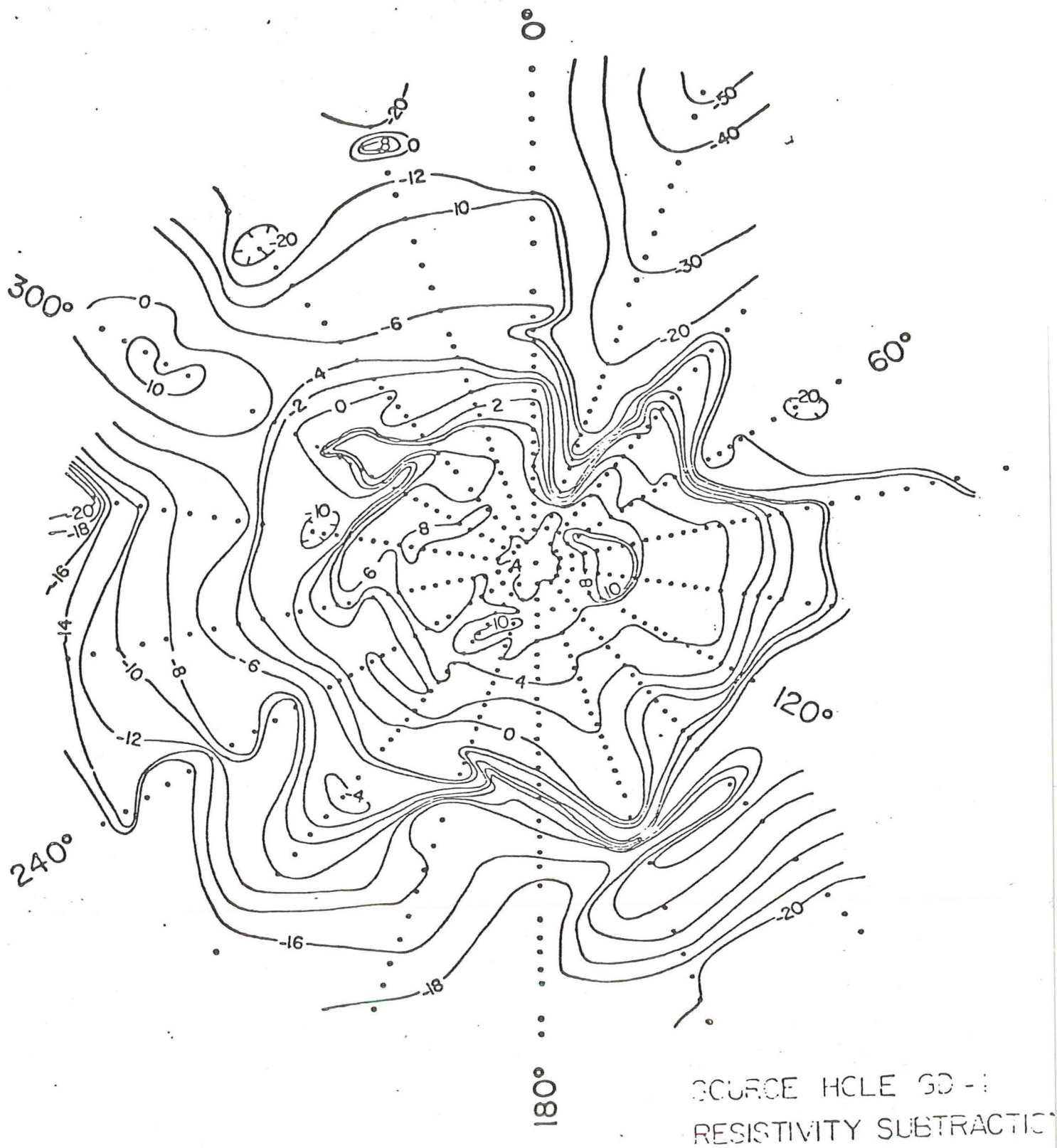518 m source depth. Contour values are in ohm-m.

Figure 15.—Resistivity subtraction-reduction map for source depths of 762 m and 1524 m. Contour values are computed by subtracting the apparent resistivity values for the 1524 m source depth from the 762 m source depth. Contour values are in ohm-m.

of anomalous zones. Most of the anomalies in figure 15 are negative (higher resistivity for the lower zone) and may indicate variations in the salt thickness. The most prominent of these anomalies is a trough-like anomaly trending along the 20° line. A possible extension of this anomaly may also be present along the 220° line. Another anomaly of note is present between the 120° and 180° lines. These anomalies will be discussed in the following summary interpretation.

Summary Interpretation

The data in figures 3 through 15 represent two distinct geoelectric zones: (1) the low resistivity geoelectric section above the salt layers (for source depths of 518 m and 762 m), and (2) the geoelectric section including the salt layers (for a source depth of 1524 m). The electric field maps for the current source pole above the salt-interbed layers (figures 3 and 4) illustrate a nearly circumferential contour pattern. An exception to this pattern occurs approximately along the 100°-300° profile lines, where breaks in the contour pattern occurs for both the 518 m source depth (figure 3) and the 762 m source depth (figure 4). This anomaly is accentuated along the 300° line on the apparent resistivity maps shown in figures 6 and 7, and is also present along the 120° line for the 762 m source. These anomalies are not as pronounced on the electric field map (figure 5) or the apparent resistivity map (figure 8) for the 1524 m source depth.

A pronounced resistivity anomaly is also present for each of the three sources between the 0° and 40° lines. Possible extensions of this anomaly may be seen in the vicinity of the 180° and 200° lines. There is some indication

that these high resistivity anomalies may be present for the shallow sources (figures 6 and 7) along the 340°, 0°, 20°, 40°, and 60° lines.

The resistivity subtraction-reduction, shown in figures 14 and 15, suggests the presence of a high resistivity zone along the 300° line at station distances away from GD-1 between 1500 and 2000 m from the source. This anomaly is not present for stations close to the source when the two sources above the salt are subtracted (figure 14), but is very much in evidence for stations greater than 1500 m from drill hole GD-1 when the deeper source is subtracted from the shallower source (figure 15). The source of the resistivity anomaly may be near the upper salt in the section and may represent a localized increase in thickness, or an upwelling of the salt. Unfortunately the extension of line 300° (line 120°) was terminated because of steep topography. However, contours along lines 80° and 140° for the deep source (figure 8) and the subtraction-reduction (figure 15) suggests the presence of an anomalous zone beyond the recorded data along line 120°.

The position of resistivity anomalies along lines 0°-to-80° vary for each of the source depths but the trend of all of these anomalies is NE-SW. The subtraction-reduction contour maps show a shallow resistivity high along the 60° line (figure 14) and a deeper resistivity low along the 20° line (figure 15). It is possible that this complex anomaly pattern represents localized folding in the salt layers that it extends into the shallow sediments above the salt.

The major circumferential resistivity contours around GD-1 are not radially symmetric. The contour spacing in figures 7 and 8 is slightly broader to the northwest, suggesting a general northwest dip of the high resistivity salt layers.

Conclusions

The hole-to-surface resistivity measurements presented in this paper were not made under ideal conditions. The current source was in a hole containing conductive fluid, which made it impossible to assume perfect point-source conditions and make a quantitative interpretation of the data. Also, the line spacing of 20° makes it difficult to define small anomalies away from the source hole. Future studies should include measurements made along lines spaced at 10° intervals.

In spite of the adverse source conditions and the sparse measurement spacing, these data do provide a good qualitative insight into the nature of the geoelectric section. The geoelectric section does not represent a perfectly layered geoelectric section. The stratigraphic section appears to dip to the northwest. In addition, variations in resistivity indicate the presence of localized changes that may represent folding or thickening of the salt layers. These resistivity anomalies are particularly evident on the 300° line, and the line interval from 0°-to-80°.

References

Alfano, Luigi, 1962, Geoelectrical prospecting with underground electrodes: Geophys. Prosp., v. 10, no. 3, p. 290-303.

Daniels, J. J., 1977, Three dimensional resistivity and induced polarization modeling using buried electrodes: Geophysics, v. 42, no. 5, p. 1006-1019.

Daniels, J. J., 1978, Interpretation of buried electrode resistivity data using a layered earth model: Geophysics, v. 43, no. 5, p. 988-1001.

Daniels, J. J., and Scott, J. H., 1980, Hole-to-surface resistivity measurements at Salt Valley, Utah: U.S. Geological Survey Open-File Report 80-981.

Merkel, R. H., and Alexander, S. S., 1971, Resistivity analysis for models of a sphere in a halfspace with buried current sources: Geophys. Prosp., v. 19, no. 4, p. 640-651.

Snyder, D. D., and Merkel, R. M., 1973, Analytic models for the interpretation of electrical surveys using buried current electrodes: Geophysics, v. 38, p. 513-529.